Catalysis Communications 51 (2014) 77–81

Contents lists available at ScienceDirect

Catalysis Communications

journal homepage: www.elsevier.com/locate/catcom

Short Communication

Enhancing the catalytic activity of carbon nanotubes by filled iron nanowires for selective oxidation of ethylbenzene

Jin Luo [a,b], Hao Yu [b], Hongjuan Wang [b], Feng Peng [b,*]

[a] School of Chemistry Science and Technology, Institute of Physical Chemistry, Zhanjiang Normal University, Zhanjiang 524048, PR China
[b] School of Chemistry and Chemical Engineering, South China University of Technology, Guangzhou 510640, PR China

ARTICLE INFO

Article history:
Received 13 January 2014
Received in revised form 3 March 2014
Accepted 25 March 2014
Available online 2 April 2014

Keywords:
Heterogeneous catalysis
Carbon nanotubes
Ethylbenzene
Aerobic oxidation

ABSTRACT

Iron nanowire filled carbon nanotubes (Fe@CNTs) were synthesized by chemical vapor deposition method and employed as heterogeneous catalysts for selective oxidation of ethylbenzene to acetophenone with molecular oxygen. The results showed that filled iron nanowires efficiently enhanced the catalytic activity of CNTs, arising from improving electron transfer. Moreover, Fe@CNTs could be easily separated from the reaction mixtures by external magnet and displayed excellent stability with no significant loss of catalytic activity after six cycling reactions. The result presented herein paves the way for the development of novel carbon catalysts for the liquid phase oxidation of ethylbenzene.

1. Introduction

Recently, the selective oxidation of ethylbenzene (EB) to higher-value added product acetophenone (AcPO) has received continuous growing interest, because AcPO is used as an important intermediate for the synthesis of pharmaceuticals, perfumes and resins [1,2]. Commercially, AcPO is produced by liquid phase cobalt-catalyzed oxidation of EB using molecular oxygen with acetic acid as solvent and manganese or bromide species as promoters [3,4]. However, not only is it unfriendly to the environment but it is also difficult to separate and recycle the catalysts from the reaction mixture. Fortunately, heterogeneous catalysis can overcome these problems. Especially, ferromagnetic metal filled carbon nanotubes (CNTs) have been widely studied in catalysis owing to their unique structures and significant magnetic properties [5–7]. On the one hand, the ferromagnetic metallic encapsulates are effectively protected by CNTs from oxidation and show long-term stability [8]. On the other hand, the well-defined nanosized channels of CNTs formed by graphene layers provide an intriguing confinement environment for nanocatalysts and catalytic reactions [9]. More importantly, the confined metal nanoparticles into CNTs have already proclaimed the ability to improve the catalytic activity in several important reactions such as syngas conversion [10,11], hydrogenation [12], ammonia decomposition [13] and oxidation [6,14]. The enhancement effect was caused by electron-deficiency, that is, the curvature of CNT walls causes the π electron density of the graphene layers to shift from the concave inner to the convex outer surface, leading to an electron-deficient interior surface and an electron-enriched exterior surface [9,15]. In our previous work [14], we succeeded in using iron filled CNTs (Fe@CNTs) to catalyze the aerobic oxidation of cyclohexane in liquid phase, and demonstrated that the enhancement of activity was caused by the improved electron transfer from iron to CNTs.

Although the influence of the Fe-filling of CNTs on the catalytic properties has been described for the oxidation of cyclohexane (naphthenic hydrocarbon) for the first time, there is no report on other oxidation reaction systems [14]. Recently, we succeeded in using CNTs to catalyze the aerobic oxidation of ethylbenzene in liquid phase, and demonstrated that the electron transfer in graphene skeletons of CNTs played an important role [16]. Therefore, it is worth further proving our viewpoint in the liquid-phase selective oxidation of ethylbenzene (aromatic hydrocarbon) to acetophenone. Herein, we have further modified the electronic characteristics by filling iron nanowires into CNTs. The results showed that filled iron nanowires efficiently enhanced the catalytic activity of CNTs for aerobic oxidation of EB, arising from improving electron transfer. More importantly, Fe@CNTs could be easily separated from the reaction mixtures through applying an appropriate magnetic field, and exhibited excellent potential for industrial application of EB oxidation to AcPO. The present work clearly shows that it is generally practical to tailor the catalytic performance by tuning electronic property through filling the CNT channels with metallic iron.

2. Experimental

Fe@CNTs were prepared by chemical vapor deposition using ferrocene as catalyst and a mixture of xylene and orthodichlorobenzene (DCB) as carbon sources in a horizontal tubular quartz furnace of 8 cm

* Corresponding author. Tel./fax: +86 20 87114916.
E-mail address: cefpeng@scut.edu.cn (F. Peng).

http://dx.doi.org/10.1016/j.catcom.2014.03.031
1566-7367/

inner diameter [8,14]. Typically, the concentration of DCB in the mixture was varied from 0, 2.5, 5, 10 to 20 vol.%. Ferrocene was dissolved in the DCB/xylene mixture to form solutions with concentration of 0.1 g/mL. A quartz slide was placed in the middle of the furnace to collect CNTs. When the temperature of the reaction region reached 800 °C, the solutions were injected by a syringe pump at a rate of 5 mL/h for 3 h, accompanied with 150 sccm H_2 and 1000 sccm Ar, respectively. Cooled under Ar to room temperature prior to exposure to air, the corresponding materials were denoted as Fe@CNTs-0, Fe@CNTs-2.5, Fe@CNTs-5, Fe@CNTs-10 and Fe@CNTs-20, respectively.

To test the role of confined Fe, the unfilled CNTs were prepared by chemical vapor deposition of xylene with Fe–Mo/Al_2O_3 as a catalyst according to our previous work [17]. To remove residual Fe–Mo/Al_2O_3 catalyst, as-grown catalysts were stirred in concentrated HCl for 6 h then washed with deionized water to pH = 6–7, and dried in air at 383 K overnight, denoted as CNTs-W. The iron content of CNTs–W was 3.4% by thermal gravimetric analysis (TGA). We also loaded FeO_x on the CNTs–W to prepare Fe/CNTs–W with 7.8% Fe.

The BET specific surface areas of the prepared samples were measured by N_2 adsorption at liquid N_2 temperature in an ASAP 2010 analyzer. Fe content was measured by thermo gravimetric analysis (Netzsch, STA449C) in air from 30 to 800 °C at a ramping rate of 10 °C/min. Raman spectra were obtained in a LabRAM Aramis micro Raman spectrometer excitated at 633 nm with 2 μm spot size. XRD patterns were recorded on a Bruker D8 ADVANCE diffractometer which was equipped with a rotating anode using Cu Kα radiation (40 kV, 40 mA). SEM images were obtained in a LEO 1530VP scanning electron microscope. TEM images were obtained in a JEM-2010 microscope operating at 200 kV. XPS analysis was performed with a Kratos Axis ultra (DLD) spectrometer equipped with an Al Kα X-ray source, the binding energies (±0.2 eV) were referenced to the C_{1s} peak at 284.6 eV.

The catalytic aerobic oxidation of EB was carried out according to our previous work [16]. Typically, the oxidation reactions were conducted in a Teflon-lined 100 mL stainless-steel autoclave equipped with a magnetic stirrer at 1100 rpm. EB (5 mL) and CH_3CN (30 mL) as the solvent, and anisole (1 mL) as an internal standard were added into the autoclave, and the reactor was flushed with argon to remove air. Then, the reactor was heated to a stable operational temperature; subsequently, pure O_2 was fed into the reactor, and the pressure was kept constant by supplying pure O_2 during the reaction. The products were identified by a Shimazdu GCMS-QP2010 detector and quantitated by Agilent GC-6820 equipped with a 30 m × 0.25 mm × 0.25 μm HP-5 capillary column and a flame ionization detector. It is worth noting that the yield of 1-phenyl-ethyl-hydroperoxide (PEHP) could not be directly measured by GC because of its thermal stability. According to literature [18,19], PEHP can be converted quantitatively to 1-phenyl-ethyl alcohol (PEA) with excessive Ph_3P at room temperature. Furthermore, for the test of reusability, the used catalyst was recovered from the reaction mixture by an external magnetic force, washed orderly with deionized water, ethanol and acetone, and dried in air. The experimental results of oxidation reaction were repeated two times, the mean data were shown. The range of experimental errors was about ±5%.

3. Results and discussion

3.1. Characterization of catalysts

Fig. 1 shows the SEM and TEM images of the synthesized catalysts. Without DCB, a well-aligned CNT array was obtained, while added DCB resulted in random orientation of CNTs. TEM images reveal that some CNTs were partially filled with long continuous Fe nanowires and the filling ratio of Fe dramatically increased with the content of DCB in the precursors increasing. Surprisingly, almost no Fe nanoparticles were attached on the outer surface of CNTs.

Fig. 2(a) depicts the XRD patterns of the synthesized catalysts. The main diffraction peaks in the $10° < \theta < 70°$ can be assigned to α-Fe, γ-Fe and graphite structure of CNTs [20,21]. It indicates that Fe nanowires in synthesized samples are composed of α-Fe and γ-Fe phases. Fig. 2(b) shows the TGA profiles of the synthesized catalysts. No remarkable weight loss occurs before 500 °C in air, demonstrating that they possess high thermal stability and the content of amorphous

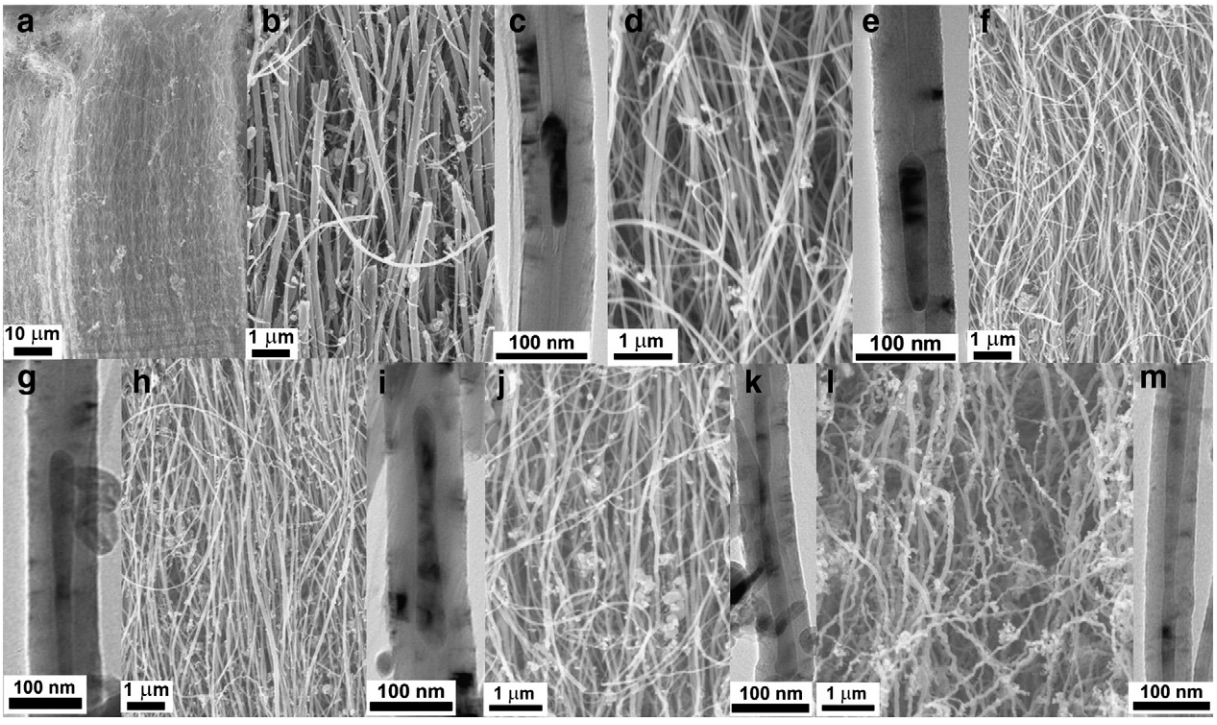

Fig. 1. SEM (a, b, d, f, h, j and l) and TEM (c, e, g, i, k and m) images of the Fe@CNTs (a, b and c), Fe@CNTs-2.5 (d and e), Fe@CNTs-5 (f and g), used Fe@CNTs-5 for 6th cycle (h and i), Fe@CNTs-10 (j and k) and Fe@CNTs-20 (l and m).

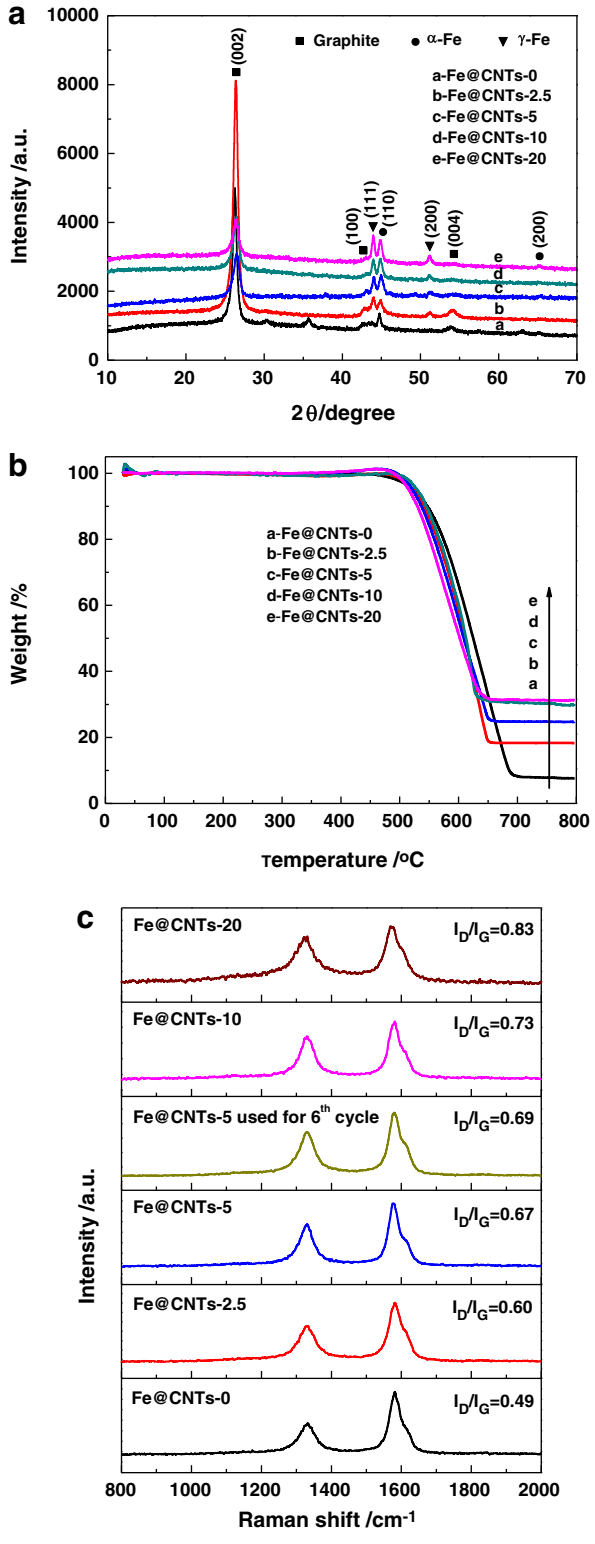

Fig. 2. XRD patterns (a), TGA patterns (b) and Raman spectra (c) of the synthesized catalysts.

carbon soot can be neglected. It is noted that the Fe residue after TGA is in the form of Fe_2O_3 and the content of Fe sharply increased with DCB from 0% to 10%. However, further increasing the DCB concentration did not contribute to the increase of Fe content. Fig. 2(c) shows two characteristic Raman peaks at approximately 1570 cm^{-1} (G-band) and 1320 cm^{-1} (D-band). The intensity ratio of D-band to G-band, namely, I_D/I_G, is used to evaluate the defects of carbon-based

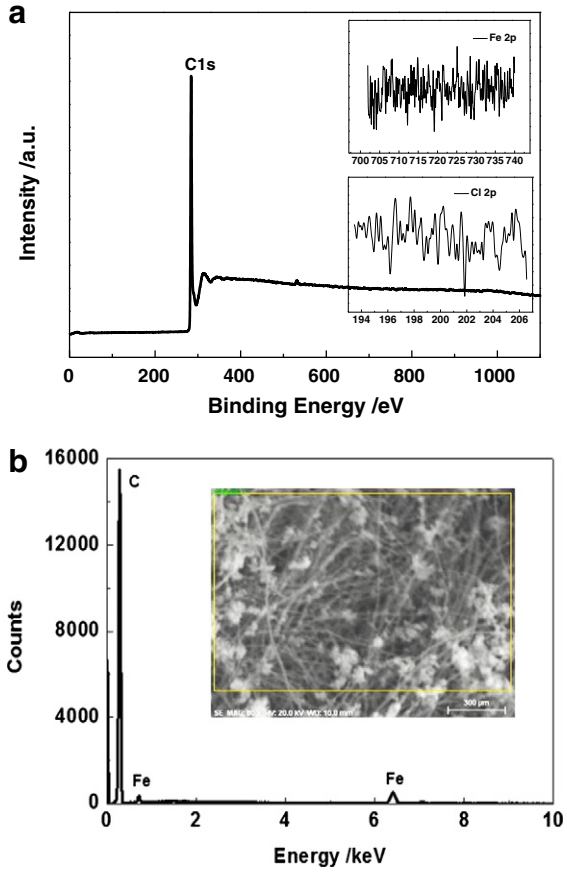

Fig. 3. The XPS survey spectrum (a) and SEM–EDS result (b) of the Fe@CNTs-5.

nanostructures [22]. The higher I_D/I_G ratio implies more defects in the carbon-based nanostructures. It was noted that the I_D/I_G ratio increased with increasing Fe content, indicating that the tubes present lattice defects and disorders derived from Fe filled in the channel of CNTs.

Fig. 3(a) shows the XPS survey spectrum of the Fe@CNTs-5. It is observed that there are no Fe and Cl on CNT surfaces, indicating that most of the iron are encapsulated in CNTs. Moreover, Fig. 3(b) shows the SEM–EDS result of the Fe@CNTs-5. It is confirmed that the nanotubes contain Fe and C, indicating that Cl is not part of the final CNT structure.

3.2. Oxidation of ethylbenzene

In our previous work [16], we have reported that CNTs could successfully catalyze the oxidation of EB with molecular oxygen, and demonstrated that the supported Fe species on the surface of CNTs did not contribute to the activity. The main products are AcPO, PEA, PEHP, benzaldehyde (BA) and benzoic acid (BzA). Table 1 compares the catalytic performances of the different carbon catalysts. The blank experiment without carbon catalyst gives an EB conversion of 9.2% with 57.2% selectivity for PEHP as the main product at 155 °C for 3 h, as a result of the autoxidation reaction [23]. Surprisingly, the Fe@CNTs-0 exhibited much higher activity than the CNTs-W, which was not filled Fe nanoparticles according to our previous work [17]. In particular, the initial specific surface activity of Fe@CNTs-0 was 2.4 times as high as that of the unfilled CNTs (Table 1, E2 and 4). Moreover, compared with the unfilled CNTs, Fe@CNTs-0 obtained much higher selectivity for AcPO and lower selectivity for PEHP. It is indicated that filled Fe nanowires can accelerate the PEHP decomposition to AcPO and indeed contribute to the considerable improvement of activity due to improving electron transfer from Fe nanowires to the CNTs. It was

Table 1
Properties and catalytic performances of the synthesized catalysts.

Entry	Catalyst	Fe (wt.%)[a]	S_{BET} ($m^2\ g^{-1}$)	I_D/I_G	r_w[b]	Conv. (%)	Selectivity (%)				
							AcPO	PEA	PEHP	BA	BzA
1	–[c]	–	–	–	–	9.2	17.9	16.3	57.2	8.6	0
2	CNTs-W	3.4	45.7	1.01[d]	0.05	28.6	55.3	9.1	11.9	11.1	12.6
3	Fe/CNTs-W	7.8	49.5	1.06[d]	0.05	28.3	53.9	9.7	10.1	12.9	13.4
4	Fe@CNTs-0	6.4	32.9	0.49	0.12	29.4	59.5	6.6	1.1	10.1	22.7
5	Fe@CNTs-2.5	12.8	30.1	0.60	0.16	31.8	59.8	5.4	0.8	11.8	22.2
6	Fe@CNTs-5	17.3	25.9	0.67	0.25	36.8	60.2	5.9	0.6	12.2	21.1
7	Fe@CNTs-5[e]	16.9	–	0.69	–	36.7	59.5	7.8	0.2	9.8	22.7
8	SiO_2/Al_2O_3–Mn[f]	–	274	–	–	53	74	26	–	–	–
9	SiO_2/Al_2O_3–Mn[g]	–	274	–	–	67	87	–	–	5	8
10	SiO_2/Al_2O_3–Co[h]	–	281	–	–	69	92	–	–	6	–
11	TPFPPCo[i]	–	–	–	–	38.6	94	5.9			
12	Fe@CNTs-10	20.9	20.3	0.73	0.20	30.4	58.2	8.7	1.9	11.5	19.7
13	Fe@CNTs-20	21.8	18.5	0.83	0.18	25.2	53.5	11.2	5.9	12.9	16.5

Reaction condition: 30 mL CH_3CN, 5 mL EB, 100 mg catalyst, 1.5 MPa O_2, 155 °C, 3 h, EB conversion and main product selectivity were determined by GC.
[a] TGA data, refers to metal iron.
[b] Initial rate of EB consumption per m^2 of catalyst surface at 1 h, $mmol \cdot m^{-2} \cdot h^{-1}$.
[c] Without catalyst.
[d] Ref. [17].
[e] The used Fe@CNTs-5 for the 6th cycle.
[f] Ref. [27]: 100 mg SiO_2/Al_2O_3–Mn (SiO_2/Al_2O_3-trimethoxysilylpropyl amine-bipyridyl ketone-Mn), 5 mL acetic acid, 2 mmol EB, 15 mol% NHPI, 100 °C, 8 h.
[g] Ref. [28]: 50 mg SiO_2/Al_2O_3–Mn (SiO_2/Al_2O_3-trimethoxysilyl propyl amine-bipyridyl ketone-Mn), 2 mmol EB, EB/TBHP (80% aqueous solution) mole ratios of 1/5, 100 °C, 24 h.
[h] Ref. [29]: 5 mg SiO_2/Al_2O_3–Co (SiO_2/Al_2O_3-trimethoxysilyl propyl amine-bipyridyl ketone-Co), 2 mmol EB, 2 mmol TBHP (80% aqueous solution), 80 °C, 24 h.
[i] Ref. [30]: 2 mL EB, 2 mol catalyst, 1.5 MPa O_2, 100 °C, 24 h.

reported that this electron transfer on the CNTs could lead to a high electron density and a decreased local work function on the carbon surface [14,24,25], which accelerated the decomposition of the most important intermediate PEHP through the π–π interaction between the PEHP and graphene sheets of the CNTs, consequently increasing the overall conversion rate.

To further prove the role of confined Fe, Fe/CNTs–W catalyst was prepared and compared. Although the Fe content of Fe/CNTs–W was 1.22 times as high as that of Fe@CNTs-0, the initial specific surface activity of Fe@CNTs-0 was 2.4 times as high as that of the Fe/CNTs–W (Table 1, E3 and 4). The result clearly indicates that the enhancement of catalytic activity was not caused by the supported Fe species on the surface of CNTs but arose from the confined Fe nanowires into CNTs.

Interestingly, the filled Fe content significantly affects the catalytic behavior of Fe@CNT catalysts. When Fe content increased from 6.4% to 17.3%, the conversion of EB at 3 h was elevated from 29.4% to 36.8%, corresponding to an increase of initial specific surface activity by 2.1 folds, and the AcPO selectivity kept stable (Table 1, E4 and 6), strongly implied that properly filling Fe nanowires into the CNTs has indeed contributed to the considerable improvement of activity. However, when Fe content further increased from 17.3% to 21.8%, the specific activity was decreased from 0.25 to 0.18, indicating that further increasing Fe content could not elevate the activity. It is probable that the increased defects in graphene sheets with the increased Fe content resulted in a decrease of conductivity and electron mobility [26] or an increase of the work function of Fe@CNTs [14], which suppressed charge transfer.

The magnetic separation and recycling of the Fe@CNTs-5 catalyst were investigated as shown in Fig. 4. Fe@CNTs-5 could be easily recovered from the reaction mixture by an external magnetic force, and showed outstanding recyclability. During six cycling tests, there was almost no difference in both the conversion of EB and selectivity for AcPO. As shown in Figs. 1 and 2(c), it is observed that the morphology and I_D/I_G ratio of the used catalyst were unchanged obviously after 6 cycles. It indicates that Fe@CNTs-5 are promising heterogeneous catalysts for industrial application of EB oxidation to AcPO.

Moreover, we also compared with other reported catalysts such as N-hydroxyphthalimide (NHPI) and $SiO_2/Al_2O_3^-$ supported manganese catalyst [27], nano-sized SiO_2/Al_2O_3 mixed oxides supported nano-Mn [28] or nano-Co(II) [29] and fluorinated metalloporphyrins [30]. The results shown in Table 1 indicated that their activities were higher than that of carbon-based catalysts but the Fe@CNTs-5 catalyst revealed more favorable potential for industrial application because NHPI is a difficult homogeneous catalyst to separate, a supported metal catalyst is easy to leach in the presence of acidic medium while fluorinated metalloporphyrins are expensive and deactivated by irreversible dimerization and it is not easy to recover the catalyst at the end of the reaction for reuse, and TBHP as oxidant is expensive and leads to new impurity. However, it still should pay more endeavors to improve the catalytic activity of carbon-based catalyst for EB oxidation to AcPO.

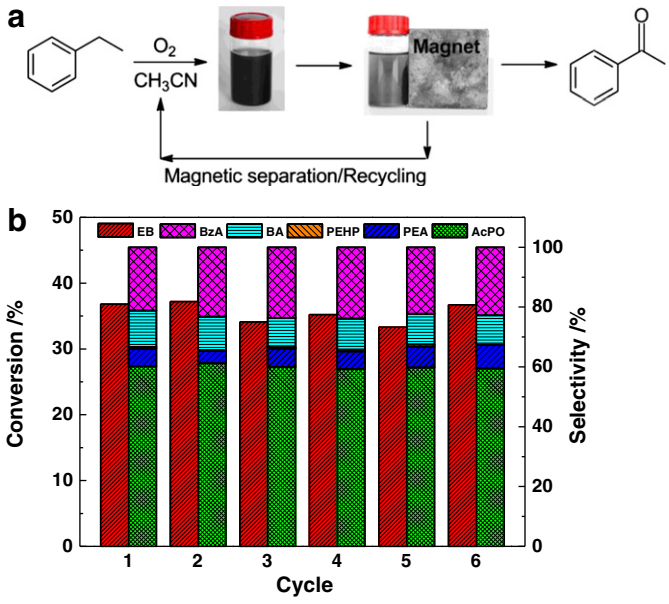

Fig. 4. Magnetic separation (a) and recyclability (b) of the Fe@CNTs-5 in liquid-phase EB oxidation.

4. Conclusions

In summary, we have demonstrated a magnetically recyclable and efficient Fe@CNT catalyst for the oxidation of EB with molecular oxygen. The results reveal that an excellent activity was obtained by filling CNTs with about 17 wt.% Fe nanowires, and filled Fe nanowires into CNTs indeed contribute to the considerable improvement of activity, arising from improving electron transfer. Moreover, Fe@CNTs could be easily recovered from the reaction mixture by an external magnetic force, and showed excellent reusability after consecutive 6 cycles with no significant loss of catalytic activity. This study exhibits the promising potential application for the liquid phase oxidation of EB to AcPO.

Acknowledgments

This work was supported by the National Natural Science Foundation of China (Nos. 21133010 and 21273079), Jiangsu Provincial Science and Technology Project (No. BE2012127), the Program for New Century Excellent Talents in Universities of China (NCET-12-0190), the Research Fund of the Guangdong Provincial Key Laboratory of Green Chemical Product Technology (GC201205) and Zhanjiang Normal University Natural Science Foundation for the Ph.D. Start-up Program (ZL1308).

References

[1] S. Devika, M. Palanichamy, V. Murugesan, Appl. Catal. A Gen. 407 (2011) 76–84.
[2] M. Arshadi, M. Ghiaci, A. Rahmanian, H. Ghaziaskar, A. Gil, Appl. Catal. B Environ. 119–120 (2012) 81–90.
[3] W. Partenheimer, Catal. Today 23 (1995) 69–158.
[4] J.Y. Qi, H.X. Ma, X.J. Li, Z.Y. Zhou, M.C.K. Choi, A.S.C. Chan, Q.Y. Yang, Chem. Commun. (2003) 1294–1295.
[5] E.C. Linganiso, G. Chimowa, P.J. Franklyn, S. Bhattacharyya, N.J. Coville, Mater. Chem. Phys. 132 (2012) 300–308.
[6] Z.Q. Shi, Z.P. Dong, J. Sun, F.W. Zhang, H.L. Yang, J.H. Zhou, X.H. Zhu, R. Li, Chem. Eng. J. 237 (2014) 81–87.
[7] H.X. Yang, S.Q. Song, R.C. Rao, X.Z. Wang, Q. Yu, A.M. Zhang, J. Mol. Catal. A Chem. 323 (2010) 33–39.
[8] W.X. Wang, K.L. Wang, R.T. Lv, J.Q. Wei, X.F. Zhang, F.Y. Kang, J.G. Chang, Q.K. Shu, Y. Q. Wang, D.H. Wu, Carbon 45 (2007) 1127–1129.
[9] X.L. Pan, X.H. Bao, Chem. Commun. (2008) 6271–6281.
[10] W. Chen, Z.L. Fan, X.L. Pan, X.H. Bao, J. Am. Chem. Soc. 130 (2008) 9414–9419.
[11] X.L. Pan, Z.L. Fan, W. Chen, Y.J. Ding, H.Y. Luo, X.H. Bao, Nat. Mater. 6 (2007) 507–511.
[12] E. Castillejos, P.J. Debouttière, L. Roiban, A. Solhy, V. Martinez, Y. Kihn, O. Ersen, K. Philippot, B. Chaudret, P. Serp, Angew. Chem. Int. Ed. 48 (2009) 2529–2533.
[13] J. Zhang, J.O. Müller, W.Q. Zheng, D. Wang, D.S. Su, R. Schlögl, Nano Lett. 8 (2008) 2738–2743.
[14] X.X. Yang, H. Yu, F. Peng, H.J. Wang, ChemSusChem 5 (2012) 1213–1217.
[15] X.L. Pan, X.H. Bao, Acc. Chem. Res. 44 (2011) 553–562.
[16] J. Luo, F. Peng, H. Yu, H.J. Wang, W.X. Zheng, ChemCatChem 5 (2013) 1578–1586.
[17] J. Luo, F. Peng, H.J. Wang, H. Yu, Catal. Commun. 39 (2013) 44–49.
[18] G.Y. Yang, Y.F. Ma, J. Xu, J. Am. Chem. Soc. 126 (2004) 10542–10543.
[19] H. Ma, J. Xu, Q.H. Zhang, H. Miao, W.H. Wu, Catal. Commun. 8 (2007) 27–30.
[20] W. Chen, Z.L. Fan, L. Gu, X.H. Bao, C.L. Wang, Chem. Commun. 46 (2010) 3905–3907.
[21] Q.F. Liu, Z.G. Chen, B.L. Liu, W.C. Ren, F. Li, H.T. Cong, H.M. Cheng, Carbon 46 (2008) 1892–1902.
[22] M.S. Dresselhaus, G. Dresselhaus, R. Saito, A. Jorio, Phys. Rep. 409 (2005) 47–99.
[23] I. Hermans, J. Peeters, P.A. Jacobs, J. Org. Chem. 72 (2007) 3057–3064.
[24] D.H. Deng, L. Yu, X.Q. Chen, G.X. Wang, L. Jin, X.L. Pan, J. Deng, G.Q. Sun, X.H. Bao, Angew. Chem. Int. Ed. 52 (2013) 371–375.
[25] R.B. Rakhi, X. Lim, X. Gao, Y. Wang, A.T.S. Wee, K. Sethupathi, S. Ramaprabhu, C.H. Sow, Appl. Phys. A 98 (2010) 195–202.
[26] H. Ago, T. Kugler, F. Cacialli, W.R. Salaneck, M.S.P. Shaffer, A.H. Windle, R.H. Friend, J. Phys. Chem. B 103 (1999) 8116–8121.
[27] D. Habibi, A.R. Faraji, M. Arshadi, H. Veisi, A. Gil, J. Mol. Catal. A Chem. 382 (2014) 41–54.
[28] D. Habibi, A.R. Faraji, Appl. Surf. Sci. 276 (2013) 487–496.
[29] D. Habibi, A.R. Faraji, C.R. Chim. 16 (2013) 888–896.
[30] X.G. Li, J. Wang, R. He, Chin. Chem. Lett. 18 (2007) 1053–1056.